

Multi-soliton solutions, breather-like and bound-state solitons for complex modified Korteweg-de Vries equation in optical fibers

Zhong-Zhou Lan(兰中周)

Citation: Chin. Phys. B, 2024, 33 (**6**): 060201. DOI: 10.1088/1674-1056/ad39d7
Journal homepage: http://cpb.iphy.ac.cn; http://iopscience.iop.org/cpb

What follows is a list of articles you may be interested in

Higher-dimensional Chen—Lee—Liu equation and asymmetric peakon soliton

Qiao-Hong Han(韩巧红) and Man Jia(贾曼)
Chin. Phys. B, 2024, 33 (**4**): 040202. DOI: 10.1088/1674-1056/ad1822

Diverse soliton solutions and dynamical analysis of the discrete coupled mKdV equation with 4×4 Lax pair

Xue-Ke Liu(刘雪珂) and Xiao-Yong Wen(闻小永)
Chin. Phys. B, 2023, 32 (**12**): 120203. DOI: 10.1088/1674-1056/acf122

Soliton interactions and asymptotic state analysis in a discrete nonlocal nonlinear self-dual network equation of reverse-space type

Cui-Lian Yuan(袁翠连) and Xiao-Yong Wen(闻小永)
Chin. Phys. B, 2021, 30 (**3**): 030201. DOI: 10.1088/1674-1056/abc2ba

Multi-soliton solutions for the coupled modified nonlinear Schrödinger equations via Riemann-Hilbert approach

Zhou-Zheng Kang(康周正), Tie-Cheng Xia(夏铁成), Xi Ma(马茜)
Chin. Phys. B, 2018, 27 (**7**): 070201. DOI: 10.1088/1674-1056/27/7/070201

Painlevé integrability of generalized fifth-order KdV equation with variable coefficients: Exact solutions and their interactions

Xu Gui-Qiong (徐桂琼)
Chin. Phys. B, 2013, 22 (**5**): 050203. DOI: 10.1088/1674-1056/22/5/050203

Multi-soliton solutions, breather-like and bound-state solitons for complex modified Korteweg–de Vries equation in optical fibers

Zhong-Zhou Lan(兰中周)†

School of Computer Information Management, Inner Mongolia University of Finance and Economics, Hohhot 010070, *China*

(Received 16 March 2024; revised manuscript received 28 March 2024; accepted manuscript online 3 April 2024)

Under investigation in this paper is a complex modified Korteweg–de Vries (KdV) equation, which describes the propagation of short pulses in optical fibers. Bilinear forms and multi-soliton solutions are obtained through the Hirota method and symbolic computation. Breather-like and bound-state solitons are constructed in which the signs of the imaginary parts of the complex wave numbers and the initial separations of the two parallel solitons are important factors for the interaction patterns. The periodic structures and position-induced phase shift of some solutions are introduced.

Keywords: complex modified KdV equation, multi-soliton solutions, breather-like, bound-state

PACS: 02.30.Ik, 02.30.Jr, 05.45.Yv, 04.20.Jb **DOI:** 10.1088/1674-1056/ad39d7

1. Introduction

Nonlinear evolution equations have been used to describe the nonlinear physical phenomena in such fields as fluid mechanics, plasma physics, optical fibres, and solid state physics.[1–9] In the shallow water, internal solitary waves can be described by the Korteweg–de Vries (KdV) equation to the first order.[10–14] A useful variant of the KdV equation is the extended KdV (eKdV)[15]

$$\eta_t + (c_0 + \alpha_1\eta + \alpha_2\eta^2)\eta_x + \beta_1\eta_{xxx} = 0, \tag{1}$$

where $\eta(x,t)$ is the wave amplitude related to the isopycnic vertical displacement, t is the time variable, x is the spatial variable in the direction of wave propagation, the coefficients α_1, α_2, and β_1 are functions of the steady background stratification and shear through the linear eigenmode of interest, the linear phase speed c_0 is the eigenvalue of the Sturm–Louiville problem for the eigenmode, while the subscripts denote the partial derivatives.[16]

For a two-layer fluid, the coefficients of Eq. (1) in the Boussinesq approximation are[17]

$$\begin{aligned} c_0 &= \sqrt{\frac{h\rho h_1 h_2}{(h_1+h_2)}}, \\ \alpha_1 &= \frac{3c_0(h_1-h_2)}{2h_1h_2}, \\ \alpha_2 &= \frac{3c_0}{h_1^2h_2^2}\left[\frac{7(h_1-h_2)^2}{8} - \left(\frac{h_1^3+h_2^3}{h_1+h_2}\right)^2\right], \\ \beta_1 &= \frac{c_0h_1h_2}{6}, \end{aligned} \tag{2}$$

where h denotes the gravitational acceleration, ρ is the relative density difference between the two layers, and h_1 and h_2 are the thicknesses of the upper layer and the lower layer, respectively. General relations for the coefficients with continuous stratification and shear can be found in Ref. [18]. In certain stratification, with certain critical combinations of the fluid density parameters, the quadratic nonlinear coefficient α_1 is equal to zero, and the eKdV equation is reduced to the modified KdV (mKdV) equation[19–21]

$$u_t + 6u^2u_x + u_{xxx} = 0, \tag{3}$$

where $u(x,t)$ is the function of the scaled coordinates x and t, and the subscript denotes derivative. The complex mKdV equation describing the propagation of optical pulses is written as[22–25]

$$u_t + 6|u|^2u_x + u_{xxx} = 0, \tag{4}$$

where u is the envelope of the electric field, x is the propagation distance, and t is the retarded time. The superregular breathers for Eq. (4) have been studied,[22] and such formations have been demonstrated also in the vector field.[23] Multi-soliton solutions for Eq. (4) are obtained by using the Darboux transformation and the reduction technique.[24] The N-th-order rogue wave solutions for Eq. (4) are constructed by the Darboux matrix method.[25]

This paper will be structured as follows: In Section 2, bilinear forms and multi-soliton solutions for Eq. (4) will be constructed through the Hirota method and symbolic computation, and the velocity of the soliton will be derived employing the concept of characteristic line. In Section 3, breather-like and bound-state solitons for Eq. (4) will be generated from the interactions of two stationary solitons, and the initial separation of the two stationary solitons will be found to be a factor that affects the interaction patterns between two stationary solitons. In Section 4, an intrinsic periodical mechanism in

†Corresponding author. E-mail: zhongzhou-lan@buaa.edu.cn

© 2024 Chinese Physical Society and IOP Publishing Ltd

the two-soliton solutions for Eq. (4) will be found analytically, and the concept of position-induced phase shift will be introduced, which can be interpreted via the asymptotic analysis. Our conclusions will be given in Section 5.

2. Bilinear forms and multi-soliton solutions for Eq. (4)

In order to detect the form of linearizable representation for Eq. (4), a transformation

$$q(x,t)=\frac{g}{f}, \tag{5}$$

will be introduced, where f is a real function of x and t, while g is a complex one. Substituting expression (5) into Eq. (4), the bilinear forms for Eq. (4) will be obtained as

$$D_x^2 f\cdot f-2g\cdot g^*=0,\quad D_t g\cdot f+D_x^3 g\cdot f=0, \tag{6}$$

where the Hirota D-operator is defined as[26]

$$D_x^{n_1}D_t^{n_2}p\cdot q=\left(\frac{\partial}{\partial x}-\frac{\partial}{\partial x'}\right)^{n_1}\times\left(\frac{\partial}{\partial t}-\frac{\partial}{\partial t'}\right)^{n_2}p(x,t)\,q(x',t')\Big|_{x'=x,t'=t}, \tag{7}$$

$p(x,t)$ is a function of x and t, $q(x',t')$ is a function of the formal variables x' and t', while n_1 and n_2 are all the non-negative integers.

In order to obtain the soliton solutions for Eq. (4), f and g are expended with respect to a small parameter ε as

$$\begin{aligned} f&=1+\varepsilon^2 f_2+\varepsilon^4 f_4+\cdots,\\ g&=\varepsilon g_1+\varepsilon^3 g_3+\varepsilon^5 g_5+\cdots, \end{aligned} \tag{8}$$

where f_ℓ ($\ell=2,4,\ldots$) are the real functions of x and t, while g_ℓ are the complex ones.

Truncating expressions (8) as

$$f=1+\varepsilon^2 f_2,\quad g=\varepsilon g_1, \tag{9}$$

and substituting expressions (9) into bilinear forms (6) with $\varepsilon=1$, the one-soliton solutions are obtained as

$$q=\frac{g_1}{1+f_2}, \tag{10}$$

where

$$\begin{aligned} &f_2=A\,\mathrm{e}^{\xi+\xi^*},\quad g_1=\mathrm{e}^{\xi},\quad \xi=kx+\omega t+\zeta,\\ &A=\frac{1}{(\omega+\omega^*)^2},\quad \omega=-k^3, \end{aligned}$$

with the wave number k, the phase ω, and the free phase constant ζ as the complex constants.

Without loss of generality, if we take ζ as zero and $k=a+b\mathrm{i}$ (a and b are real constants), the intensity of the soliton can be derived as

$$|u|^2=\frac{\mathrm{e}^{2a(-a^2t+3b^2t+x)}}{\left[1+\dfrac{\mathrm{e}^{2a(-a^2t+3b^2t+x)}}{4a^2}\right]^2}. \tag{11}$$

In order to derive the velocity of the soliton, we employ the concept of characteristic line for the solitonic propagation. Characteristic-line equation can be written as

$$2a(-a^2t+3b^2t+x)=\text{const}. \tag{12}$$

Differentiating Eq. (12) on both sides with respect to t, we obtain the velocity of the soliton as

$$v=a^2-3b^2. \tag{13}$$

Thus, $v<0$ the left-propagating solitons, $v>0$ corresponds to the right-propagating solitons, and $v=0$ the stationary solitons, which are shown in Fig. 1.

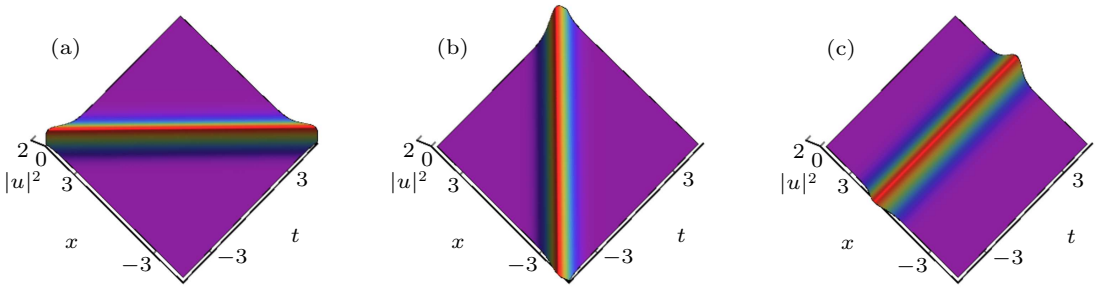


Fig. 1. Propagation of one solitons via Eq. (11) with $\zeta=0$: (a) $\sqrt{2}+\mathrm{i}$; (b) $\sqrt{2}+\frac{\sqrt{3}}{3}\mathrm{i}$; (c) $\sqrt{2}+\frac{\sqrt{6}}{3}\mathrm{i}$.

Next, truncating expressions (8) as

$$f=1+\varepsilon^2 f_2+\varepsilon^4 f_4,\quad g=\varepsilon g_1+\varepsilon^3 g_3, \tag{14}$$

and substituting expressions (14) into bilinear forms (6) with $\varepsilon=1$, the two-soliton solutions are obtained as

$$q=\frac{g_1+g_3}{1+f_2+f_4}, \tag{15}$$

where

$$\begin{aligned} &g_1=\mathrm{e}^{\xi_1}+\mathrm{e}^{\xi_2},\quad g_3=A_{123}\,\mathrm{e}^{\xi_1+\xi_2+\xi_1^*}+A_{124}\,\mathrm{e}^{\xi_1+\xi_2+\xi_2^*},\\ &f_2=A_{13}\,\mathrm{e}^{\xi_1+\xi_1^*}+A_{23}\,\mathrm{e}^{\xi_2+\xi_1^*}+A_{14}\,\mathrm{e}^{\xi_1+\xi_2^*}+A_{24}\,\mathrm{e}^{\xi_2+\xi_2^*},\\ &f_4=A_{1234}\,\mathrm{e}^{\xi_1+\xi_1^*+\xi_2+\xi_2^*},\\ &\xi_j=k_jx+\omega_jt+\zeta_j,\quad \omega_j=-k_j^3,\\ &A_{12}=(\omega_1-\omega_2)^2,\quad A_{34}=(\omega_1^*-\omega_2^*)^2,\\ &A_{j,l+2}=\frac{1}{(\omega_j+\omega_j^*)^2},\quad A_{123}=A_{12}A_{13}A_{23},\\ &A_{124}=A_{12}A_{14}A_{24},\quad A_{1234}=A_{12}A_{13}A_{14}A_{23}A_{24}A_{34}, \end{aligned}$$

with k_l, ω_l, and ζ_l as the complex constants, $j,l=1,2$.

3. Breather-like and bound-state solitons for Eq. (4)

The breather-like soliton solution for Eq. (4) can be derived via certain choices of parameters in the two-soliton solutions (15). The first prerequisite for the formation of breather-like solitons is that the two solitons have to be parallel, i.e., they travel in the same direction with the same speed. Another is that the two parallel solitons have to be comparable in energy, i.e., their difference of amplitude should not be too large, which can be achieved by taking fairly close values for the complex wave numbers k_1 and k_2. It is also found that the signs of the imaginary parts of k_1 and k_2 have to be opposite for breather-like solitons to form. Another crucial factor that affects the formation of the breather-like solitons is the initial separation of the two solitons, which can be adjusted by virtue of setting different values to ζ_1 and ζ_2.

The formation of breather-like solitons is depicted in Fig. 2, when the initial separation of the two stationary solitons is gradually reduced. If the initial separation is big enough, i.e., the two solitons are separated well apart, there is little mutual interactions between the two solitons in Fig. 2(a). As we can see in Fig. 2(b), the mutual attractions cause periodic oscillations and produce conjunctival bandages between the two soltions, when the two stationary solitons are drawn closer. From Fig. 2(c), we can observe that the oscillations become bigger and more energy pools into the conjunctive bandage, when the two stationary solitons are initiated even closer to each other. Finally, as seen in Fig. 2(d), when the initial separation of the two stationary solitons is small enough, the two solitons interact strongly, and the soliton profiles are broken periodically, while the conjunctive bandages merge into the breather-like solitons.

From Fig. 3, when k_1 and k_2 are set to be complex conjugates, and ζ_1 and ζ_2 are set to be 0, solutions (15) becomes real, and the breather-like solitons of the real mKdV equation can be derived.

Different from the breather-like solitons, the signs of the imaginary parts of k_1 and k_2 have to be the same for the bound-state solitons. When the two stationary solitons are separated well apart, the two stationary solitons have little mutual interactions as seen in Fig. 4(a). From Fig. 4(b), we can find that there are periodic oscillations, when the two stationary solitons are drawn closer. The tendency that the two parallel solitons attract and repulse each other is clear, and it should be noted that the period of the oscillations in the case for the bound-state solitons here is much larger then that in the case for the breather-like solitons in Fig. 2(b). In Fig. 4(c), the bound-state soliton is formed, and the two stationary solitons attract and repulse each other with energy peaks forming periodically. Proper adjustments in the phase constants ζ_1 and ζ_2 can make the bound-state solitons in more symmetrical patterns as shown in Fig. 4(d), in which case, the amplification in the energy peaks is more remarkable than the asymmetric case.

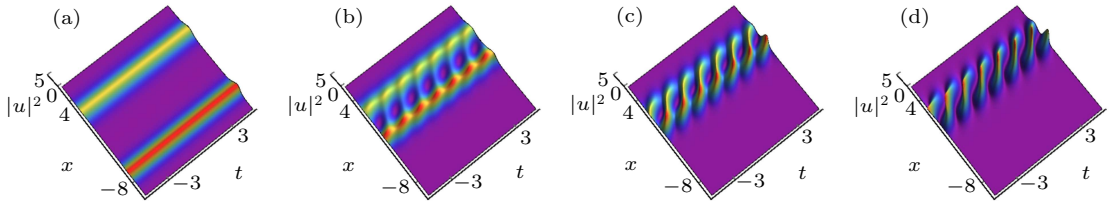


Fig. 2. Interactions between two stationary solitons via Eq. (15) with $k_1 = \frac{6}{5} - \frac{3\sqrt{2}}{5}\mathrm{i}$, $k_2 = 1 + \frac{\sqrt{3}}{3}\mathrm{i}$, $\zeta_2 = 0$: (a) $\zeta_1 = 9$; (b) $\zeta_1 = 3$; (c) $\zeta_1 = \frac{6}{5}$; (d) $\zeta_1 = 0$.

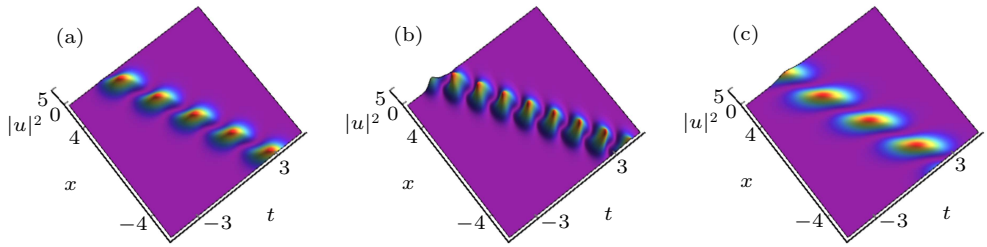


Fig. 3. mKdV breather-like solitons via Eq. (15) with $\zeta_1 = \zeta_2 = 0$: (a) $k_1 = \frac{\sqrt{2}}{2} - \mathrm{i}$ and $k_2 = \frac{\sqrt{2}}{2} + \mathrm{i}$; (b) $k_1 = 1 - \mathrm{i}$ and $k_2 = 1 + \mathrm{i}$; (c) $k_1 = \frac{1}{2} - \mathrm{i}$ and $k_2 = \frac{1}{2} + \mathrm{i}$.

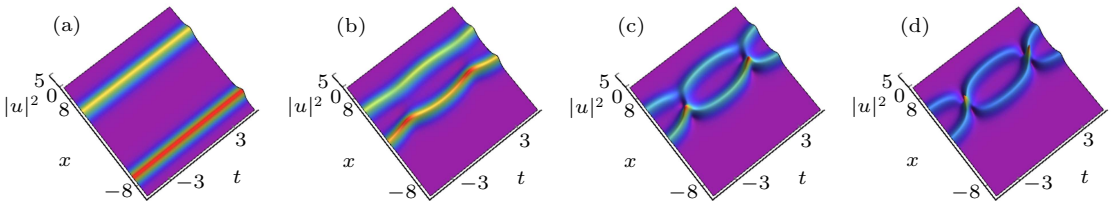


Fig. 4. Interactions of two stationary solitons via Eq. (15) with $k_1 = \frac{6}{5} + \frac{3\sqrt{2}}{5}\mathrm{i}$, $k_2 = 1 + \frac{\sqrt{3}}{3}\mathrm{i}$, $\zeta_2 = 0$: (a) $\zeta_1 = 9$; (b) $\zeta_1 = 1$; (c) $\zeta_1 = 0$; (d) $\zeta_1 = -\frac{2}{5}$.

4. Periodic structures and position-induced phase shift

Taking $k_1 = a_1 + b_1\mathrm{i}$ and $k_2 = a_2 + b_2\mathrm{i}$ to emphasize the periodic property, we can rewrite Eq. (15) as

$$u = \frac{\mathrm{e}^{\mathrm{i}\Phi_1+\phi_1}Q_1 + \mathrm{e}^{\mathrm{i}\Phi_2+\phi_2}Q_2}{D + 2r\mathrm{e}^{\Theta_1+\Theta_2+\theta_1+\theta_2}\cos(\Phi_1-\Phi_2+\phi_1-\phi_2+\varphi)}, \tag{16}$$

where

$$\begin{aligned}
&Q_1 = \mathrm{e}^{\Theta_1+\theta_1} + B_{12}\mathrm{e}^{2\Theta_2+\Theta_1+2\theta_2+\theta_1},\\
&Q_2 = \mathrm{e}^{\Theta_2+\theta_2} + B_{11}\mathrm{e}^{2\Theta_1+\Theta_2+2\theta_1+\theta_2},\\
&D = 1 + A_{11}\mathrm{e}^{2\Theta_1+2\theta_1} + A_{12}\mathrm{e}^{2\Theta_2+2\theta_2} + C_{11}\mathrm{e}^{2\Theta_1+2\Theta_2+2\theta_1+2\theta_2},\\
&B_{11} = r_1\mathrm{e}^{\mathrm{i}\varphi_1}, \quad B_{12} = r_2\mathrm{e}^{\mathrm{i}\varphi_2},\\
&\Theta_j = a_j[x + (3b_j^2 - a_j^2)t],\\
&\Phi_j = b_j[x + (b_j^2 - 3a_j^2)t], \quad \theta_j = \mathrm{Re}(\zeta_j),\\
&\phi_j = \mathrm{Im}(\zeta_j), \quad A_{13} = r\mathrm{e}^{\mathrm{i}\varphi},
\end{aligned}$$

and $j = 1, 2$, a_1, a_2, b_1, b_2 are real numbers, while $\mathrm{Re}(z)$ and $\mathrm{Im}(z)$ are the real and imaginary parts of z, respectively. The intensity of u can be expressed as

$$|u|^2 = \frac{|Q_1|^2 + |Q_2|^2 + 2P}{[D + 2r\chi\cos(\rho+\varphi)]^2}, \tag{17}$$

with

$$\begin{aligned}
\chi &= \mathrm{e}^{\Theta_2+\Theta_1+\theta_2+\theta_1}, \quad \rho = \Phi_1 - \Phi_2 + \phi_1 - \phi_2,\\
P &= \chi\cos\rho + r_1\mathrm{e}^{3\Theta_1+3\theta_1}\cos(\rho-\varphi_1)\\
&\quad + r_2\mathrm{e}^{3\Theta_2+3\theta_2}\cos(\rho+\varphi_2)\\
&\quad + r_1r_2\chi^2\cos(\rho+\varphi_2-\varphi_1).
\end{aligned}$$

In the case of two stationary solitons, from Eq. (13), we have $a_i^2 = 3b_j^2$, so

$$\begin{aligned}
\Phi_1 - \Phi_2 &= (b_1-b_2)x + (b_1^2 - b_2^2 - 3a_1^2 + 3a_2^2)t\\
&= (b_1-b_2)x + 8(b_2^3 - b_1^3)t,
\end{aligned} \tag{18}$$

from which the period of the periodic behavior can be expressed as

$$\Gamma = \frac{2\pi}{|b_1(b_1^2-3a_1^2) - b_2(b_2^2-3a_2^2)|} = \frac{2\pi}{8|b_1^3 - b_2^3|}. \tag{19}$$

From Eq. (19), it can be seen that when the absolute values of b_1 and b_2 are close enough, the signs of them can significantly alter the value of the period Γ. In Fig. 2, they take the opposite sign, then the period is $\Gamma = 0.288$, which is much smaller than the case in Fig. 4, where the period is $\Gamma = 1.079$. This is in agreement with the phenomenon that the period of oscillations in Fig. 4 is much bigger than that in Fig. 2. When the absolute values of them are in big disparity, the different signs will not make big difference in the period, and the interactions of two stationary solitons can exhibit breather-like patterns in Figs. 5(a) and 5(b). Moreover, when the absolute values of them are in medium disparity, periodic structures between the breather-like and bound-state solitons can be generated in Fig. 5(c).

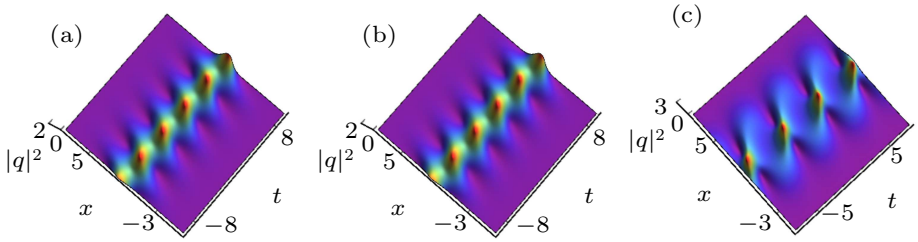


Fig. 5. Interactions of two stationary solitons and periodic structures via Eq. (15) with (a) $k_1 = \frac{1}{5} + \frac{3\sqrt{3}}{15}\mathrm{i}$, $k_2 = 1 + \frac{\sqrt{3}}{3}\mathrm{i}$, $\zeta_1 = -\frac{4}{5}$, and $\zeta_2 = 0$; (b) $k_1 = \frac{1}{5} - \frac{3\sqrt{3}}{15}\mathrm{i}$, $k_2 = 1 + \frac{\sqrt{3}}{3}\mathrm{i}$, $\zeta_1 = -\frac{21}{25}$, and $\zeta_2 = 0$; (c) $k_1 = \frac{1}{2} + \frac{\sqrt{3}}{6}\mathrm{i}$, $k_2 = 1 + \frac{\sqrt{3}}{3}\mathrm{i}$, $\zeta_1 = \zeta_2 = 0$.

From Fig. 6, we can see an obvious phase difference in the 1st soliton, when the the position of the 2nd soliton is changed from the far right of the 1st soliton to the far left. Because this phase shift is caused by the relative position of the two solitons, we call it the position-induced phase shift. This phenomenon can be interpreted via the asymptotic analysis. When the 2nd soliton is positioned at the far right of the 1st soliton, $\theta_2 \to -\infty$, and

$$|u|^2 \to \left(\frac{\mathrm{e}^{\Theta_1+\theta_1}}{1 + A_{11}\mathrm{e}^{2\Theta_1+2\theta_1}}\right). \tag{20}$$

When the 2nd soliton is positioned at the far left of the 1th soliton, $\theta_2 \to \infty$, and

$$|u|^2 \to \left(\frac{\mathrm{e}^{\Theta_1+\theta_1+\Delta\phi_\mathrm{p}}}{1 + A_{11}\mathrm{e}^{2\Theta_1+2\theta_1+2\Delta\phi_\mathrm{p}}}\right), \tag{21}$$

where the position-induced phase shift $\Delta\phi_\mathrm{p}$ can be determined from

$$\Delta\phi_\mathrm{p} = \frac{(a_1-a_2)^2 - (b_1-b_2)^2}{(a_1+a_2)^2 + (b_1-b_2)^2}, \tag{22}$$

and $\Delta\phi_\mathrm{p} < 0$ as $a_1a_2 > 0$.

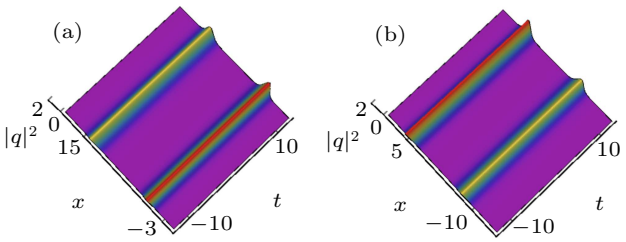


Fig. 6. Position-induced phase shift of the stationary solitons via Eq. (15) with $k_1 = \frac{6}{5} + \frac{2\sqrt{3}}{5}\mathrm{i}$, $k_2 = 1 + \frac{\sqrt{3}}{3}\mathrm{i}$, $\zeta_1 = 0$: (a) $\zeta_2 = -8$, (b) $\zeta_2 = 8$.

5. Conclusions

In this paper, a complex mKdV equation which describes propagation of short pulses in optical fibers, i.e., Eq. (4), has been investigated. Bilinear forms and multi-soliton solutions for Eq. (4) have be constructed through the Hirota method and symbolic computation. The breather-like and bound-state solitons for Eq. (4) have been constructed with the interactions between two parallel solitons. We have found that the signs of the imaginary parts of the complex wave numbers and the initial separation of the two parallel solitons are important for the interaction patterns. With the decreasing of the separation between the two parallel solitons, their mutual interaction gradually strengthens and in this process different interaction patterns can be observed in Figs. 2–4. An intrinsic periodical mechanism has been found analytically via rewriting the two-soliton solution (15) as solution (16). The breather-like and bound-state solitons can be interpreted with the periodical mechanism in Fig. 5. The concept of position-induced phase shift has been introduced, which can be seen in Fig. 6.

Acknowledgements

Project supported by the National Natural Science Foundation of China (Grant No. 12161061), the Fundamental Research Funds for the Inner Mongolia University of Finance and Economics (Grant No. NCYWT23036), the Young Innovative and Entrepreneurial Talents of the Inner Mongolia Grassland Talents Project in 2022, Autonomous Region "Five Major Tasks" Research Special Project for the Inner Mongolia University of Finance and Economics in 2024 (Grant No. NCXWD2422), High Quality Research Achievement Cultivation Fund for the Inner Mongolia University of Finance and Economics in 2024 (Grant No. GZCG2426), and the Talent Development Fund of Inner Mongolia Autonomous Region, China.

References

[1] Zhou Q 2022 *Chin. Phys. Lett.* **39** 010501
[2] Liu C, Chen S C, Yao X K and Akhmediev N 2022 *Chin. Phys. Lett.* **39** 094201
[3] He J T, Fang P P and Lin J 2022 *Chin. Phys. Lett.* **39** 020301
[4] Ding C C, Zhou Q, Xu S L, Triki H and Mirzazadeh M and Liu W J 2023 *Chin. Phys. Lett.* **40** 040501
[5] Yan L J, Liu Y J and Hu X B 2024 *Chin. Phys. Lett.* **41** 040201
[6] Wazwaz A M 2023 *Chin. Phys. Lett.* **40** 120501
[7] Liu X M, Zhang Z Y and Liu W J 2023 *Chin. Phys. Lett.* **40** 070501
[8] Ma W X 2022 *Chin. Phys. Lett.* **39** 100201
[9] Lou S Y, Jia M and Hao X Z 2023 *Chin. Phys. Lett.* **40** 020201
[10] Lamb K G, Xiao W and Kurkin A 2007 *Phys. Rev. E* **75** 046306
[11] Zhu S Y, Kong D X and Lou S Y 2023 *Chin. Phys. Lett.* **40** 080201
[12] Yuan F and Ghanbari B 2023 *Chin. Phys. B* **32** 040201
[13] Chen M and Wang Z 2023 *Chin. Phys. B* **32** 090504
[14] Kruglov V I and Triki H 2023 *Chin. Phys. Lett.* **40** 090503
[15] Helfrich K R and Melville W K 2006 *Annu. Rev. Fluid Mech.* **38** 395
[16] Sasa N and Satsuma J 1991 *J. Phys. Soc. Jpn.* **60** 409
[17] Lamb K G, Yan L 1996 *J. Phys. Ocean.* **26** 2712
[18] Grimshaw R, Pelinovsky E and Poloukhina O 2002 *Nonlinear Proc. Geophys.* **9** 221
[19] Modak1 S, Singh A P and Panigrahi P K 2016 *Eur. Phys. J. B* **89** 149
[20] Chen J B and Pelinovsky D E 2019 *J. Nonlinear Sci.* **29** 2797
[21] Chowdury A, Ankiewicz A and Akhmediev N 2016 *Eur. Phys. J. D* **70** 104
[22] Liu C, Ren Y, Yang Z Y and Yang W L 2017 *Chaos* **27** 083120
[23] Liu C, Chen S C and Akhmediev N 2024 *Phys. Rev. Lett.* **132** 027201
[24] Zhaqilao and Li Z B 2008 *Chin. Phys. Lett.* **25** 8
[25] Zhaqilao 2013 *Phys. Scr.* **87** 065401
[26] Hirota R 1973 *J. Math. Phys.* **14** 805